Structures of the Cu_4MgPh_6 and $[Cu_4LiPh_6]^-$ Clusters: First Example of a Magnesium-Containing Transition-Metal Cluster Compound

Saeed I. Khan, Peter G. Edwards,[1] Hanna S. H. Yuan, and Robert Bau*

Contribution from the Department of Chemistry, University of Southern California, Los Angeles, California 90089. *Received September 17, 1984*

Abstract: The first structural characterization of a transition-metal cluster complex containing magnesium, Cu_4MgPh_6, is reported in this paper, together with its lithium analogue, $[Cu_4LiPh_6]^-$. Both have the same basic trigonal-bipyramidal geometry that has been detected earlier in other M_5Ph_6 clusters: $[Cu_5Ph_6]^-$, $[Cu_3Li_2Ph_6]^-$, and $[Ag_3Li_2Ph_6]^-$. The six phenyl groups bridge the M(axial)–M(equatorial) bonds in a perpendicular fashion, while the M(eq)···M(eq) distances are nonbonding. Judging from the large number of isolated complexes that have this common structure, one can speculate that the trigonal bipyramid may be the thermodynamically most stable geometry in M/M′/Ph systems (M = Cu, Ag; M′ = Li, Mg) (at least for unsubstituted phenyl ligands). Crystallographic details: $[Cu_4LiPh_6]^-[Li(Et_2O)_4]^+\cdot 2Et_2O$ crystallizes in the trigonal space group $P31c$, with $a = b = 13.242$ (3) Å, $c = 19.343$ (5) Å, $V = 2939$ (1) Å^3, $Z = 2$, ρ(calcd) = 1.16 g cm^{-3}, and a final R factor = 0.103 for 550 reflections. $Cu_4MgPh_6\cdot Et_2O$ crystallizes in the triclinic space group $P\bar{1}$, with $a = 10.394$ (2) Å, $b = 10.480$ (4) Å, $c = 9.909$ (4) Å, $\alpha = 107.86$ (3)°, $\beta = 96.56$ (2)°, $\gamma = 111.25$ (2)°, $V = 926.2$ (5) Å^3, $Z = 1$, ρ(calcd) = 1.47 g cm^{-3}, and a final R factor = 0.049 for 2920 reflections.

As part of a program to structurally characterize metal cluster complexes of unsubstituted phenyl ligands, we have recently reported the structures of the $[Cu_5Ph_6]^-$ and $[Ag_3Li_2Ph_6]^-$ anions.[2,3] Concurrently, the closely related $[Cu_3Li_2Ph_6]^-$ has been described by Hope et al.[4] In this paper we extend out studies to the Cu_4MgPh_6 and $[Cu_4LiPh_6]^-$ clusters.

Experimental Section

Cu_4MgPh_6 was prepared from CuBr and $MgPh_2$ with the method of Seitz and Madl.[5] Attempts to grow crystals of this compound were hindered by its limited solubility in common organic solvents. However, crystals of a quality suitable for X-ray analysis could be obtained simply by cooling the dark-green mother liquor which remains after the pale yellow product has been filtered off. Crystals of $Cu_4MgPh_6\cdot Et_2O$ grow as yellow prisms, tinged with a light-green hue. They crystallize in the non-centric space group $P\bar{1}$ (No. 1; triclinic), with unit cell parameters $a = 10.394$ (2) Å, $b = 10.480$ (4) Å, $c = 9.909$ (4) Å, $\alpha = 107.86$ (3)°, $\beta = 96.56$ (2)°, $\gamma = 111.25$ (2)°, $V = 926.2$ (5) Å^3, $Z = 1$, and ρ(calcd) = 1.47 g/cm^{-3}. Data were collected at room temperature, using a Nicolet/Syntex $P2_1$ diffractometer with Mo Kα radiation. The structure was solved[6] by heavy-atom methods: a Patterson map was used to locate the four Cu atoms, and difference-Fourier syntheses were used to locate the other non-hydrogen atoms in the molecule. Full-matrix least-squares refinement led to a final agreement factor of $R = 0.049$ for 2920 nonzero reflections with $I > 3\sigma(I)$.

$[Cu_4LiPh_6]^-$ was prepared from CuBr and LiPh in a manner closely analogous to that for $[Cu_5Ph_6]^-$: To a cooled (−20 °C) suspension of copper bromide (1 g, 7 mmol) in diethyl ether (50 mL) was added, dropwise with vigorous stirring, a solution of phenyllithium (14.4 mL, 0.017 M in Et_2O, 14 mmol). After the addition, the yellow suspension was allowed to warm slowly, through 0 °C when the solution become clear yellow, to room temperature. After being stirred for about 1 h, the yellow solution was filtered, concentrated in vacuo until crystals started to appear, and held overnight at −20 °C. The resulting white crystals of LiBr were filtered off, and the supernatant was further concentrated and cooled as before, yielding pale yellow prisms of $[Cu_4LiPh_4]^-[Li(Et_2O)_4]^+\cdot 2Et_2O$. In contrast to Cu_4MgPh_6, which is stable indefinitely at room temperature, salts of $[Cu_4LiPh_6]^-$ are thermally unstable, decomposing at room temperature in several days.

Pale-yellow prisms of $[Cu_4LiPh_6]^-[Li(Et_2O)_4]^+\cdot 2Et_2O$ crystallize in the trigonal space group $P31c$ (No. 159), with $a = b = 13.242$ (3) Å, $c = 19.343$ (5) Å, $\alpha = \beta = 90°$, $\gamma = 120°$, $V = 2939$ (1) Å^3, $Z = 2$, and ρ(calcd) = 1.16 g cm^{-3}. Data were collected in the manner described earlier. The structure was solved by heavy-atom methods and refined[6] to a final agreement factor of $R = 0.103$ for 550 nonzero reflections.[7] The relatively high agreement factor is largely due to severe disorder problems affecting some of the ether carbon atoms.[8] The $[Cu_4LiPh_6]^-$ anion, however, refined well.

Table I. Average Distances and Angles in $Cu_4MgPh_6\cdot Et_2O$

(A) Distances (in Å)	
Cu(ax)—Cu(eq)	2.427 (2)
Cu(eq)···Cu(eq)	3.019 (3)
Cu(ax)···Mg	3.828 (4)
Cu(eq)—Mg	2.754 (4)
Cu(ax)—C	2.09 (1)
Cu(eq)—C	1.95 (1)
Mg—C	2.35 (1)
Mg—O	2.046 (9)
(B) Angles (in deg)	
Cu(eq)–Cu(ax)–Cu(eq)	76.72 (5)
Cu(ax)–Cu(eq)–Mg	95.06 (9)
Cu(eq)–Mg–Cu(eq)	66.30 (9)
Cu(ax)–C–Cu(eq)	73.1 (3)
Cu(eq)–C–Mg	79.0 (4)
C–C(ax)–C	119.7 (4)
C–Cu(eq)–C	160.9 (4)
C–Mg–C	117.1 (4)

Description and Discussion of the Structures

A plot of the Cu_4MgPh_6 cluster is shown in Figure 1, and selected distances and angles given in Table I. A list of final atomic coordinates is available.[9] This compound represents, to

(1) Current address: Chemistry Department, University College, P.O. Box 78, Cardiff CF1 1XL, U.K.

(2) Edwards, P. G.; Gellert, R. W.; Marks, M. W.; Bau, R. *J. Am. Chem. Soc.* **1982**, *104*, 2072.

(3) Chiang, M. Y.; Böhlen, E.; Bau, R. *J. Am. Chem. Soc.*, preceding paper in this issue.

(4) Hope, H.; Oram, D.; Power, P. *J. Am. Chem. Soc.* **1984**, *106*, 1149.

(5) Seitz, L. M.; Madl, R. *J. Organomet. Chem.* **1972**, *34*, 415.

(6) Most of the major computations in this work were performed with CRYM, an amalgamated set of crystallographic programs developed by Dr. R. E. Marsh and co-workers at the California Institute of Technology. For the least-squares refinement of $[Cu_4LiPh_6]^-$, the rigid-body program UCIGLS was used, adapted by R. J. Doedens and J. A. Ibers from W. R. Busing and H. A. Levy's ORFLS least-squares refinement program.

(7) Because of the small number of reflections, the phenyl groups are refined as rigid bodies.

(8) The details of the disorder of the ether molecules are as follows: The $[Li(Et_2O)_4]^+$ cation is situated on a crystallographic three-fold (C_3) rotation axis, passing through the Li and one of the O atoms. The three *off-axis* ether molecules are ordered, with all oxygen and carbon atoms located and refined. The fourth oxygen atom (situated on the C_3 axis) necessarily has to have disordered carbon atoms, since Et_2O clearly does not have threefold symmetry. Numerous weak peaks around the vicinity of that O atom could be seen, but could neither be unambiguously assigned nor successfully refined. The same situation exists for the two ether molecules of crystallization, whose oxygen atoms also lie on crystallographic C_3 axes.

(9) See supplementary material paragraph at end of paper for ordering details.

0002-7863/85/1507-1682$01.50/0

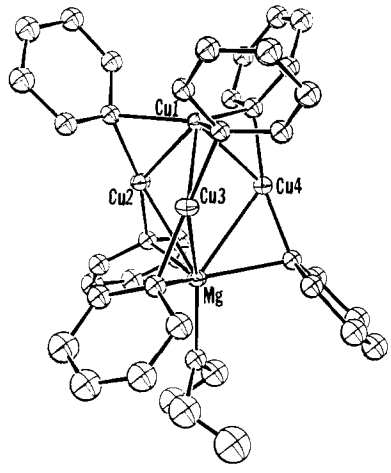

Figure 1. Molecular plot of $Cu_4MgPh_6 \cdot Et_2O$.

Table II. Average Distances and Angles in $[Cu_4LiPh_6]^-$

(A) Distances (in Å)	
Cu(ax)—Cu(eq)	2.55 (3)
Cu(eq)···Cu(eq)	3.31 (2)
Cu(ax)···Li	3.34 (5)
Cu(eq)—Li	2.52 (3)
Cu(ax)—C	2.33 (3)
Cu(eq)—C	1.96 (4)
Li—C	2.16 (4)
(B) Angles (in deg)	
Cu(eq)-Cu(ax)-Cu(eq)	80.8 (2)
Cu(ax)-Cu(eq)-Li	82.4 (9)
Cu(eq)-Li-Cu(eq)	81.9 (9)
Cu(ax)-C-Cu(eq)	72.1 (14)
Cu(eq)-C-Li	75.7 (16)
C-Cu(ax)-C	119.6 (11)
C-Cu(eq)-C	168.1 (18)
C-Li-C	119.7 (16)

our knowledge, the first example[10] of a transition-metal cluster complex containing a magnesium atom (or any member of the magnesium family) structurally characterized. Note that, unlike $[Cu_5Ph_6]^-$,[2] $[Ag_3Li_2Ph_6]^-$,[3] $[Cu_3Li_2Ph_6]^-$,[4] or $[Cu_4LiPh_6]^-$ (vide infra), Cu_4MgPh_6 is the only member of this series containing a solvent molecule as a ligand (to Mg). This may be due to the fact that whereas in the other four compounds the axial atoms (Cu or Li) are roughly coplanar with the plane of the three ipso carbon atoms, in Cu_4MgPh_6 the Mg atom is displaced 0.4 Å away from it, making it more "exposed" to coordination by ether. This in turn may reflect the larger covalent radius of Mg compared with Li (in addition, Mg has a higher tendency to achieve tetrahedral coordination[11]). Otherwise, the geometry of Cu_4MgPh_6 is very similar to that of $[Cu_5Ph_6]^-$:[2] the six phenyl rings are all bridging and roughly perpendicular to the metal(axial)–metal(equatorial) bonds, and the M(ax)–M(eq) distances are substantially shorter (bonding) than the M(eq)···M(eq) distances (nonbonding).

A molecular plot of $[Cu_4LiPh_6]^-$ is shown in Figure 2, and selected distances and angles given in Table II. A list of final atomic coordinates is available.[9] The $[Cu_4LiPh_6]^-$ cluster is situated on a crystallographic C_3 rotation axis, as is the tetrahedral

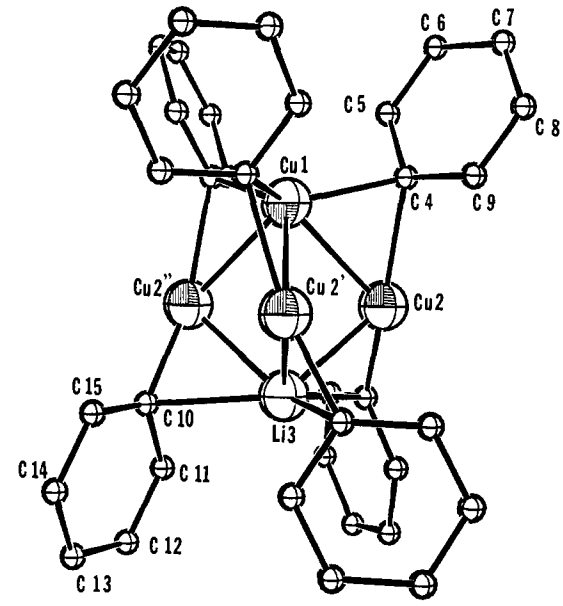

Figure 2. Molecular plot of the $[Cu_4LiPh_6]^-$ anion.

$[Li(Et_2O)_4]^+$ cation. In the anion, the C_3 axis passes through the axial atoms, Cu(1) and Li(3). Once again, the familiar trigonal-bipyramidal geometry is found, with bonding M(ax)–M(eq) distances, nonbonding M(eq)···M(eq) distances, and phenyl ligands bridging the M(ax)–M(eq) edges. Just as in the case of $[Ag_3Li_2Ph_6]^-$,[3] the Li site in $[Cu_4LiPh_6]^-$ is contaminated with a significant amount of the heavier metal: occupancy refinement revealed that the Li(3) site is composed of 89% Li and 11% Cu. From the crystallographic results alone, it is not possible to tell if this reflects a dynamic Li/Cu exchange taking place between clusters and isolated cations in solution or whether the partial occupancy simply means that $[Cu_4LiPh_6]^-$ and $[Cu_5Ph_6]^-$ are co-crystallizing together.

Organolithium cuprates and related compounds are, of course, well-known reagents in organic synthesis (as are organocopper/Grignard mixtures).[12] What the common geometry of the series $[Cu_5Ph_6]^-$, $[Cu_4LiPh_6]^-$, $[Cu_3Li_2Ph_6]^-$ (and, one might add, also $[Cu_4MgPh_6]$ and $[Ag_3Li_2Ph_6]^-$) suggests is that, at least for phenylating reagents, the basic trigonal-bipyramidal structure may in fact be one of the dominant species (perhaps the thermodynamically most stable entity) in phenyllithium–cuprate solutions. The occurrence of this same geometrical arrangement in five different structures (actually six, since $[Cu_5Ph_6]^-$ was isolated as two different salts[2]) is striking, to say the least.[13]

Alternatively, the clusters $[Cu_5Ph_6]^-$, $[Cu_4LiPh_6]^-$, $[Cu_3Li_2Ph_6]^-$, and $[Ag_3Li_2Ph_6]^-$ may be viewed as three $[MPh_2]^-$ units (M = Cu, Ag; the equatorial atoms) held together loosely by two univalent cations (M′ = Li^+ or Cu^+; the axial atoms). A similar suggestion had been made earlier in connection with the complex $Au_2Li_2(aryl)_4$.[15] The fact that Ag^+ and Cu^+ contamination has been found in the axial Li^+ sites of $[Ag_3Li_2Ph_6]^-$[2] and $[Cu_4LiPh_6]^-$[14] suggests that what may be taking place in solution is an equilibrium between $[MPh_2]^-$ monomers (presumably linear) and $[M_3M'_2Ph_6]^-$ clusters (i.e., $3[MPh_2]^- + 2[M']^+ \rightleftarrows [M_3M'_2Ph_6]^-$), with the latter perhaps being the predominant species.

(10) (a) It has come to our attention, however, that the compound $H-Ru_4(CO)_{10}(MgCH_3)$ has recently been isolated, with a $MgCH_3$ group bridging one of the edges of the Ru_4 tetrahedron (S. G. Shore, private communication to R. Bau, 1984). In addition, it should be noted that structure determinations have been reported on three other compounds containing transition-metal/magnesium bonds.[10b,10c] These compounds however, are not cluster complexes. (b) Felkin, H.; Knowles, P. J.; Meunier, B.; Mitschler, A.; Ricard, L.; Weiss, R. *Chem. Commun.* **1974**, 44. (c) Prout, K.; Forder, R. A. *Acta Crystallogr.* **1975**, *B31*, 852.

(11) (a) Weiss, E. *Chem. Ber.* **1965**, *98*, 2805. (b) Johnson, C.; Toney, J.; Stucky, G. D. *J. Organomet. Chem.* **1972**, *40*, C11. (c) Stucky, G. D.; Rundle, R. E. *J. Am. Chem. Soc.* **1968**, *90*, 5375.

(12) (a) Posner, G. H. "An introduction to Synthesis Using Organocopper Reagents"; Wiley: New York, 1980; Chapter 1. (b) Kauffman, T. *Angew. Chem., Int. Ed. Engl.* **1974**, *13*, 291. See, for example, ref 71 and 77 in this review.

(13) Just as striking is the fact that the trigonal-bipyramidal geometry of the anion persists even though the cations are widely different in all cases: $[Li(THF)_4]^+$ (ref 2), [Li(THF)(pentamethyldiethylenetriamine)]$^+$ (ref 2), $[Li(Et_2O)_4]^+$ (this work), $[Li_4Cl_2(Et_2O)_{10}]^{2+}$ (ref 4), $[Li_6Br_4(Et_2O)_{10}]^{2+}$ (ref 3); and no countercation at all in the case of Cu_4MgPh_6 (this work).

(14) This work.

(15) Van Koten, G.; Jastrzebski, J. T. B. H.; Stam, C. H.; Niemann, N. C. *J. Am. Chem. Soc.* **1984**, *106*, 1880.

Acknowledgment. We thank the National Science Foundation (Grants No. CHE-81-01122 and No. CHE-83-20484) for supporting this work.

Registry No. Cu_4MgPh_6, 94859-46-8; $Cu_4MgPh_6 \cdot Et_2O$, 94859-47-9; $[Cu_4LiPh_6]^-[Li(Et_2O)_4]^+$, 94942-21-9; $[Cu_4LiPh_6]^-[Li(Et_2O)_4]^+ \cdot 2Et_2O$, 94942-22-0; copper bromide, 11129-27-4; phenyllithium, 591-51-5.

Supplementary Material Available: The final atomic coordinates of $Cu_4MgPh_6 \cdot Et_2O$ (Table A) and $[Cu_4LiPh_6]^-[Li(Et_2O)_4]^+ \cdot 2Et_2O$ (Table B) (2 pages). Ordering information is given on any current masthead page.

Thermochromic Transformations of 2,6-Diorgano-1,3,5,7-tetraoxa-2,6-dibora-4,8-octalindiones: A Model for Solid-State Phase Transformations and Hysteresis

Mohamed Yalpani,* Walter R. Scheidt, and Klaus Seevogel

Contribution from the Max-Planck-Institut für Kohlenforschung, Kaiser-Wilhelm-Platz 1, D-4330 Mülheim an der Ruhr, West Germany. *Received June 8, 1984*

Abstract: The mechanisms underlying phase transformations and hysteresis have been investigated by using the example of the phase changes resulting from the solid-state thermochromic reactions of **1a–i**. It is found that the transition "order" is strictly dependent on the morphology of the solids used. Thus, polycrystalline samples of **1** give diffuse transitions, while with tempered and almost homogeneous crystals, nearly isothermal transitions are obtained. Pressure thermograms and substituent effects point to a generalized model for hysteresis phenomena which suggests an interdependence of the ΔH of the chemical reaction and of the ensuing lattice or conformational changes in a transforming system.

We recently described the preparation,[1] the X-ray structure analysis, and the mechanism[2] of the solid-state polymerization–depolymerization and thermochromic reaction of the boraheterocycle **1**. The cell dimensions of the single crystal of **1b**, determined between −73 and +40 °C, indicated considerable volume changes.[2] It could thus be expected that this reaction is accompanied by one or more phase changes. Furthermore we had observed a very significant hysteresis in the thermochromic temperature T_{th}. In view of the paucity of reports on fully reversible solid-state organic reactions (cf. recent reviews on organic solid-state reactions[3]), and the continued interest in this still not fully understood field of chemistry, we set out to extend our investigations on this reaction. In particular we hoped to gain insights into the mechanism of the unusually large hysteresis effects observed for the various derivatives of **1**.

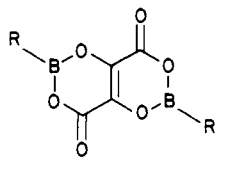

1

	R
1a	CH_3
b	C_2H_5
c	n-C_3H_7
d	i-C_3H_7
e	i-C_4H_9
f	c-C_6H_{11}
g	n-C_8H_{17}
h	n-$C_{16}H_{33}$
i	$CH_2C_6H_5$

Results

Thermal Rearrangement of 1 under a Kofler Hot-Stage Microscope. Preliminary observations of the crude crystals of **1c**, as separated from the reaction mixture, under a hot-stage microscope showed them to be thin yellow plates, some of which were hexagons of uniform size. Heating them at a rate of about 1 °C/min through the T_{th} at about +75 °C resulted in a uniform color change (yellow to colorless) within about 0.5 °C. When cooled the thermochromic change (colorless to yellow) set in at about +55 °C and was completed within 0.5 °C. In the heating and cooling cycles, no visual change of the crystal dimensions could be detected. Neither could any cracking or shattering of the crystals be observed. Also the colored (colorless) areas formed showed the same extinction direction between crossed polarized light as did the starting crystals. Sublimation of the above crude crystals gave mostly a polycrystalline mass. Under the microscope they appeared layered and twinned, and nearly all were of undefined shape. The transition of the individual polycrystals through T_{th} was no longer uniform. Color change commenced successively at different points in each layer of the polycrystals and moved across the layers as a "liquid" front (compare Figure 2 in ref 4). This process was completed within about 2 °C. When the heating and cooling cycles were retraced, the same starting points for the color change were observed in any one polycrystal.

DSC Analysis of 1. Figure 1 shows heating and cooling scans for crude crystals of **1b** and **c**, respectively. The effect of sublimation on the heating scans of **1c** is shown in Figure 2. In Figure 3 is shown that the onset temperature for the change is, over a wide range, nearly independent of the heating rate. The variations of the peak transition temperature (T_p) with applied mechanical pressure on solid **1c** and **b** are shown in Figures 4 and 5, respectively. A summary of selected results of the DSC measurements for the various derivatives of **1** is given in Table I.

Infrared Studies. Figure 6A and B shows the infrared spectra in the region of 2000–400 cm^{-1} of the high- and low-temperature forms of **1c** taken at +95 and −20 °C, respectively. Prominent among the changes are the peaks in the region between 1950 and 1500 cm^{-1}. The two peaks at 1760 and 1735 cm^{-1} of the "hot" form can be assigned to free carbonyl stretchings. In the "cold" form, these have decreased drastically and have become replaced by two bands at 1645 and 1550 cm^{-1} assignable to chelated carbonyl stretchings. Figure 6C shows the effect of sublimation on the infrared spectrum of **1c**. In Figure 7A the integrated intensities of the peaks at 1760 and 1735 cm^{-1} of sublimed crystals of **1c** through three heating and cooling cycles are plotted against temperature. This figure also clearly shows the pronounced hysteresis in the heating and cooling process. The effect of in-

(1) Yalpani, M.; Köster, R. *Chem. Ber.* **1983**, *116*, 3332.
(2) Yalpani, M.; Boese, R.; Bläser, D. *Chem. Ber.* **1983**, *116*, 3338.
(3) Paul, I. C.; Curtin, D. Y. *Acc. Chem. Res.* **1973**, *6*, 217. Gavezzotti, A.; Simonetta, M. *Chem. Rev.* **1982**, *82*, 1.
(4) McCullough, D. Y., Jr.; Curtin D. Y.; Paul, I. C. *J. Am. Chem. Soc.* **1972**, *94*, 874.

0002-7863/85/1507-1684$01.50/0